

Alma Mater Studiorum Università di Bologna  
Archivio istituzionale della ricerca

Unlocking Access to Enantiopure Fused Uracils by Chemodivergent [4+2] Cross-Cycloadditions: DFT-Supported Homo-Synergistic Organocatalytic Approach

This is the final peer-reviewed author's accepted manuscript (postprint) of the following publication:

*Published Version:*

Curti C., Rassa G., Lombardo M., Zambrano V., Pinna L., Battistini L., et al. (2020). Unlocking Access to Enantiopure Fused Uracils by Chemodivergent [4+2] Cross-Cycloadditions: DFT-Supported Homo-Synergistic Organocatalytic Approach. *ANGEWANDTE CHEMIE. INTERNATIONAL EDITION*, 59(45), 20055-20064 [10.1002/anie.202007509].

*Availability:*

This version is available at: <https://hdl.handle.net/11585/778320> since: 2020-11-06

*Published:*

DOI: <http://doi.org/10.1002/anie.202007509>

*Terms of use:*

Some rights reserved. The terms and conditions for the reuse of this version of the manuscript are specified in the publishing policy. For all terms of use and more information see the publisher's website.

This item was downloaded from IRIS Università di Bologna (<https://cris.unibo.it/>).  
When citing, please refer to the published version.

(Article begins on next page)

This is the final peer-reviewed accepted manuscript of:

**Unlocking Access to Enantiopure Fused Uracils by Chemodivergent [4+2] Cross-Cycloadditions: DFT-Supported Homo-Synergistic Organocatalytic Approach**

C. Curti, G. Rassu, M. Lombardo, V. Zambrano, L. Pinna, L. Battistini, A. Sartori, G. Pelosi, F. Zanardi

Angew. Chem. Int. Ed. 2020, 45, 20055–20064

The final published version is available online at:  
<https://doi.org/10.1002/anie.202007509>

Terms of use:

Some rights reserved. The terms and conditions for the reuse of this version of the manuscript are specified in the publishing policy. For all terms of use and more information see the publisher's website.

*This item was downloaded from IRIS Università di Bologna (<https://cris.unibo.it/>)*

***When citing, please refer to the published version.***

## Unlocking Access to Enantiopure Fused Uracils via Chemodivergent [4 + 2] Cross Cycloadditions: a DFT-Supported Homo-Synergistic Organocatalytic Approach

Claudio Curti,\*[a] Gloria Rassu,[b] Marco Lombardo,\*[c] Vincenzo Zambrano,[b] Luigi Pinna[d] Lucia Battistini,[a] Andrea Sartori,[a] Giorgio Pelosi,[e] and Franca Zanardi\*[a]

[a] Prof. Dr. C. Curti, Prof. Dr. L. Battistini, Prof. Dr. A. Sartori, Prof. Dr. F. Zanardi

Dipartimento di Scienze degli Alimenti e del Farmaco

Università di Parma

Parco Area delle Scienze 27A, 43124 Parma, Italy

E-mail: claudio.curti@unipr.it (C.C.), franca.zanardi@unipr.it (F.Z.)

[b] Dr. G. Rassu, Dr. V. Zambrano

Istituto di Chimica Biomolecolare

Consiglio Nazionale delle Ricerche

Traversa La Crucca 3, 07100 Li Punti Sassari, Italy

[c] Prof. Dr. M. Lombardo

Dipartimento di Chimica "Giacomo Ciamician"

Università di Bologna

Via Selmi 2, 40126 Bologna, Italy

E-mail: marco.lombardo@unibo.it

[d] Prof. Dr. L. Pinna

Dipartimento di Chimica e Farmacia

Università di Sassari

Via Vienna 2, 07100 Sassari, Italy

[e] Prof. Dr. G. Pelosi

Dipartimento di Scienze Chimiche, della Vita e della Sostenibilità Ambientale

Università di Parma

Parco Area delle Scienze 17A, 43124 Parma, Italy

Supporting information for this article is given via a link at the end of the document.

*This item was downloaded from IRIS Università di Bologna (<https://cris.unibo.it/>)*

***When citing, please refer to the published version.***

Abstract: The discovery of chemical methods enabling the construction of carbocycle-fused uracils which embody a three-dimensional and functional group-rich architecture is a useful tool in medchem synthesis. In this work, an unprecedented amine-catalyzed [4 + 2] cross cycloaddition is documented, which involved remotely enolizable 6-methyluracil-5-carbaldehydes and  $\alpha$ -aryl enals, and chemoselectively produced two novel bicyclic and tricyclic fused uracil chemotypes in good yields and maximum level of enantiocontrol. In-depth mechanistic investigations and control experiments support an intriguing homo-synergistic organocatalytic approach, where the same amine organocatalyst concomitantly engages both aldehyde partners in a first stepwise eliminative [4 + 2] cycloaddition, whose vinylogous iminium ion intermediate product may diverge – depending upon conditions – to either bicyclic targets via hydrolysis, or tricyclic products via a further homo-synergistic trienamine-mediated stepwise [4 + 2] cycloaddition.

## Introduction

Over the past two decades, the development of breakthrough synthetic methods, such as organocatalyzed processes and direct activation modalities of nonactivated C-H bonds, have revolutionized the way molecules are imagined and made, with enormous impact on neighboring disciplines including pharmaceutical research and chemical biology.[1] In the drug discovery field, an ever-growing demand for innovative synthesis methods is profiling, enabling the rapid construction of high-quality lead structures that merge the drug-like properties of functionalized core scaffolds with increased three-dimensional shape, thereby expanding the uncharted chemical space around the putative biological targets.[2]

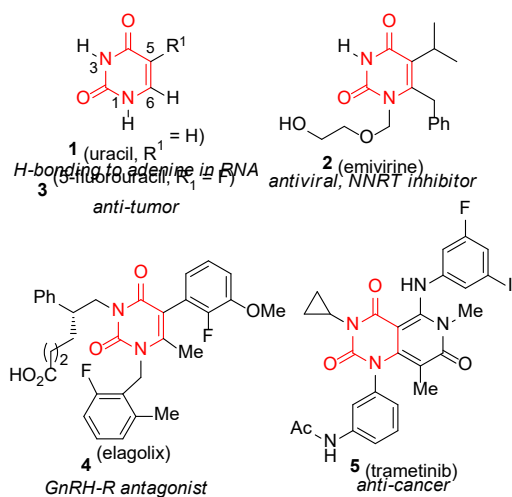
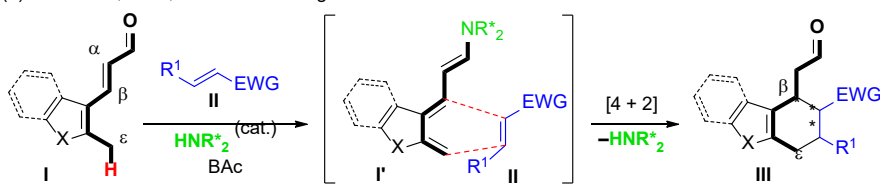


Figure 1. Uracil and uracil-based drugs. NNRT = Non-Nucleoside Reverse Transcriptase.

This item was downloaded from IRIS Università di Bologna (<https://cris.unibo.it/>)

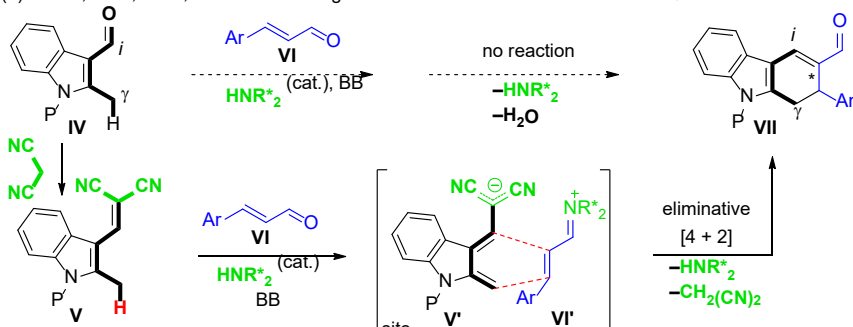
**When citing, please refer to the published version.**

(1) Melchiorre, 2011, via HOMO-raising trienamine/ $\rho$ QDM activation (ref. 9)



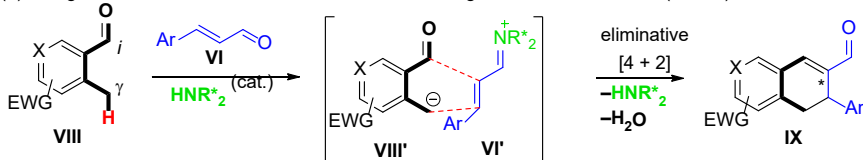
X = NBoc, O; EWG = NO<sub>2</sub>, CO<sub>2</sub>Et, COAr  
R<sup>1</sup> = Ar, COAr, indolinone; BAC = Brønsted acid

(2) Rassa, Curti, 2016, via HOMO-raising malononitrile/ $\rho$ QDM and LUMO-lowering iminium ion activation (ref. 10a)



P = Boc, Moc; BB = Brønsted base; *i* = ipso site

(3) Wang, 2013, via EWG installation and LUMO-lowering iminium ion activation (ref. 11)



X = N, C(NO<sub>2</sub>); EWG = NO<sub>2</sub>, CF<sub>3</sub>, Cl, Br

Scheme 1. Previous vinylogous C(sp<sup>3</sup>)-H functionalization strategies for the asymmetric construction of fused (hetero)cycles.

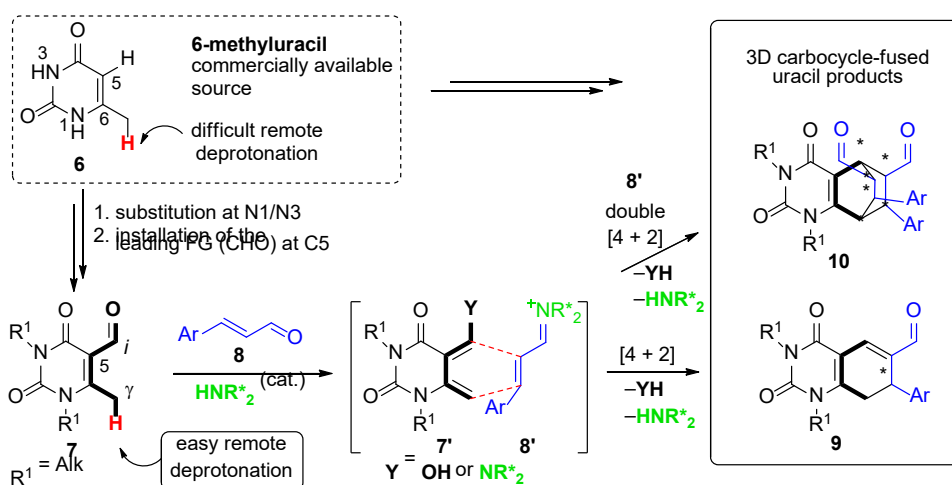
Among the privileged core motifs, the naturally occurring heterocycle uracil (compound 1, Figure 1) occupies a preeminent position, due to its innate chemical structure – a stable six-membered 2,4-pyrimidindione ring with prevalence of the lactam tautomeric form – responsible for it to establish key gene-related H-bond connections.[3] In addition, uracil has proven to be extremely inclined toward chemical modification, especially at the N1, N3, C5, and C6 positions.[4] Accordingly, a wide array of uracil-based molecules has been accessed so far, exhibiting as many diverse biological activities ranging from antiviral and anti-tumor to herbicidal, bactericidal, and anti-malarial action, as testified by the outstanding number of uracil-founded drugs approved worldwide (Figure 1).[5] Chemical modifications of the uracil ring often maintain the pyrimidindione core, which is enriched with atoms and/or flexible aromatic/aliphatic chains (e.g. compounds 2, 3, and 4), while it is possibly fused with flanking heterocycles, as in the pyridopyrimidine structure 5, which generally are flattened and C(sp<sup>2</sup>)-rich rings.[6] Rare examples of chiral uracil-fused cycles have been reported so far, which have been mainly accessed in racemic format via nonasymmetric syntheses.[5b]

This item was downloaded from IRIS Università di Bologna (<https://cris.unibo.it/>)

When citing, please refer to the published version.

Asymmetric chemical methods enabling the rapid elaboration of commercially available uracil-based materials toward chiral enantio- and functional group-enriched fused uracils is still on demand, and our aim here is to address this goal.

The application of the principle of vinylogy – which states that the electronic properties of a functional group within a molecule are possibly transmitted to a remote position through interposed conjugated multiple bonds – has become an appealing opportunity in organic synthesis for the predictable and selective functionalization of remote C(sp<sup>3</sup>)-H bonds.[7] In particular, the benzylic site of ortho-methyl (hetero)aromatic carbaldehydes IV and VIII or extended polyenals of type I (Scheme 1) may be envisaged as a remotely enolizable position of the vinylogous aldehyde system, so that useful functionalization chemistry with suitable acceptor components may be fostered. However, deprotonation of these benzylic vinylogous sites is not simple, since it generates highly reactive ortho-quinodimethane species (oQDMs) – indeed truly polyenolate donors – where the aromatic character of the original ring is temporarily lost.[8] To enhance the acidity of such benzylic protons, clever solutions were devised, as exemplified in Scheme 1. In a first example (Scheme 1, eq. 1),[9] upon condensation of aldehyde I with the amine catalyst, the activated oQDM-trienamine donor I' is formed in situ, which closes with the electron-poor olefin II to consign the [4+2]-locked fused cyclohexane product III. When a similar organocatalyzed reaction was performed using methylindole carbaldehyde IV (eq. 2), featuring a formyl function directly attached to the aromatic ring, the cross coupling with enal acceptor VI failed to produce any cyclized products, probably due to insufficient capability of the reaction system to generate the dearomatized oQDM donor. In that instance, a strategic escamotage was devised, to temporarily activate the donor carbaldehyde chemoselectively as a methylenemalonate derivative V, to trigger the intended [4 + 2] coupling between the in situ-activated components V' and VI'. The spontaneous malononitrile elimination finally provided the ipso-locked cyclohexene aldehyde products VII in a global eliminative [4 + 2] cycloaddition reaction.[10]



Scheme 2. Projected plan for the asymmetric construction of fused uracils in this work.

In the third example (Scheme 1, eq. 3), the cross-coupling between ortho-tolualdehyde VIII and enals VI could be feasible by installing electron-withdrawing groups in the donor component (i.e. nitro groups); in

This item was downloaded from IRIS Università di Bologna (<https://cris.unibo.it/>)

**When citing, please refer to the published version.**

the event, an eliminative [4 + 2] cyclization took place between VIII' and the iminium ion-activated enal partner VI'.<sup>[11]</sup>

In this work, we focus on a novel uracil scaffold, namely compound 7 (Scheme 2), which is easily equipped with an exocyclic carbaldehyde handle at C5 starting from the cheap, commercially available 6-methyluracil precursor 6. Concomitant vinylogation of the C6-methyl with both the aldehyde and the endocyclic lactam moieties would render the C-H deprotonation at C6 feasible under mild conditions. Remote  $\alpha$ -deprotonation would lead to electron-rich diene 7', which is anticipated to undergo either one single or double [4 + 2] cycloadditions with iminium ion-activated dienophile 8', to ultimately provide access to diversely shaped chiral carbocyclic uracils of type 9 and/or 10 (vide infra).

Distinguished features of this strategy are: (1) the exploitation of the unique structural motif of methyluracil carbaldehyde 7, whose scarce aromatic character would in principle facilitate formation of the putative active oQDM-type species 7';<sup>[3]</sup> (2) the perspective of generating, for the first time, new chiral, 3D space-filling fused uracils in one pot from available uracil-based precursors, representing a step forward with respect to established methods of functionalization of uracils; and (3) the possibility of introducing variable substituents at the N1/N3 atoms, thus allowing modulation of the physico-chemical properties of substrates and targets.

From a mechanistic point of view, additional interesting perspectives would open, as to define the actual role of the amine catalyst in activating either or both the aldehyde carbonyl groups of the reacting partners 7 and 8, to unveil the concerted vs stepwise nature of the cyclization reactions, as well as to unravel the intimate reasons responsible for chemodivergency toward either classes of uracil-fused products.

Our efforts in this work were directed to put this plan into practice, to demonstrate its viability with diversely substituted substrates, and to get insights into the reaction mechanism via in-depth DFT computational investigation backed up by sound experimental evidences.

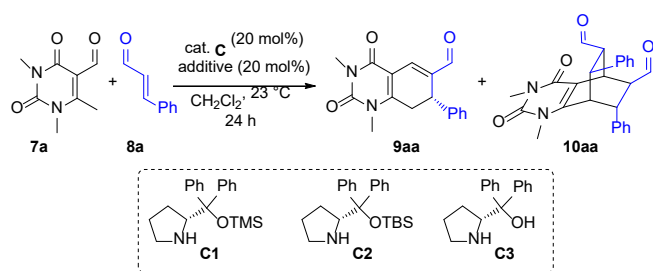
## Results and Discussion

**Synthesis.** As a proof of concept of the feasibility of the proposed plan (Scheme 2), we initially evaluated the reaction between N,N-dimethyl-substituted methyluracil carbaldehyde 7a and cinnamaldehyde (8a) under amine organocatalysis (Table 1). Compound 7a, in turn, was accessed via a two-step procedure by starting from cheap and commercially available 6-methyluracil (6) via bis-N-methylation (Me<sub>2</sub>SO<sub>4</sub>, K<sub>2</sub>CO<sub>3</sub>) followed by Vilsmeier formylation. Thus, treating 7a and 8a in an equimolar ratio in the presence of popular TMS-protected prolinol C1 (20 mol%) and catalytic DIPEA in CH<sub>2</sub>Cl<sub>2</sub>, led to the formation of carbaldehyde 9aa in 36% yield, accompanied by not negligible amounts of the tricyclic product 10aa (9% yield; Table 1, entry 1). While compound 9aa coincided exactly with our expectations according to a plausible eliminative [4 + 2] cross cycloaddition between the two substrates, compound 10aa came as a surprise, likely as the result of a double cycloadditive process involving two mol equiv of the cinnamaldehyde component (for mechanistic details, see infra). Since the very first experiment, hence, we became aware of three facts: the reaction was feasible, it could lead to two new uracil-fused chemotypes, and the enantiocontrol by secondary amine organocatalysis was absolutely excellent for both types. Accordingly, we proceeded to the systematic screening of the reaction conditions, in order to maximize both yield and chemoselectivity for either targets, while maintaining enantiocontrol.

*This item was downloaded from IRIS Università di Bologna (<https://cris.unibo.it/>)*

***When citing, please refer to the published version.***

Table 1. Proof of concept of the plan and selected optimization of reaction conditions.[a]



Entry	Cat. C	7a:8a	Additive	Yield	[b] 9aa:10aa[c]	ee [%] 9aa/10aa[d]
1	C1	1:1	DIPEA	45	4:1	99/>99
2	C2	1:1	DIPEA	30	>10:1	99/n.d.
3	C3	1:1	DIPEA	15	n.d.	n.d./n.d.
4	-	1:1	-	-	-	-
5	-	1:1	DIPEA	-	-	-
6[e]	C1	1:1	DIPEA	35	1:1	99/>99
7	C1	1:1	Et3N	40	2:1	99/>99
8	C1	1:1	-	55	5:1	99/>99
9	C1	1.5:1	-	65	10:1	99/n.d.
10[f]	C1	1.5:1	-	35	10:1	99/n.d.
11[g]	C1	1.5:1	-	15	n.d.	n.d./n.d.
12[h]	C1	1.5:1	-	30	>10:1	99/>99
13	C1	1.5:1	BA	55	1:1	99/>99
14	C1	2:1	-	74	>10:1	>99/n.d.
15	C1	1:1.5	-	45	3:1	99/>99
16	C1	1:3	BA	79	1:6	n.d./>99

[a]All reactions were run under inert atmosphere on a 0.2 mmol scale (0.1 M). [b]Combined yield of isolated products 9aa and 10aa. [c]Determined by <sup>1</sup>H NMR analysis of the crude reaction mixture.

[d]Determined by HPLC analysis on a chiral stationary phase. [e]Toluene was used. [f]0 °C and 48 h reaction time. [g]50 °C and 12 h reaction time. [h]10 mol% catalyst loading. DIPEA = N,N-diisopropylethylamine. BA = benzoic acid. n.d. = not determined. For complete optimization survey, see Tables S1-S2 in the Supporting Information.

As for the organocatalysts screened, the first catalyst used, C1, revealed to be the best one, since reactions performed with other secondary amine catalysts or tertiary amine bifunctional catalysts either gave inferior results in terms of product yield (entries 2 and 3), or proved completely non-productive (Table S1,

This item was downloaded from IRIS Università di Bologna (<https://cris.unibo.it/>)

**When citing, please refer to the published version.**



Supporting Information). No reaction took place in the absence of any amine catalyst, both in the presence or absence of the DIPEA additive, emphasizing the key role of the catalyst in triggering the transformation (entries 4 and 5). The role of solvent, additive, molar ratio between substrates, catalyst loading, and reaction temperature was next investigated (Table 1, entries 7-16 and Table S2 in the Supporting Information), ultimately leading to the following conclusions. First, chemodivergency, i.e. 9aa:10aa ratio, was strictly dependent by the 7a:8a substrate ratio, with bicycle 9aa prevailing with excess of 7a over 8a, and tricycle 10aa predominating with excess 8a over 7a. Second, the role of the additive crucially impacted both yield and chemoselectivity; in fact, the absence of any added Brønsted base or acid improved the overall efficiency of the reaction toward the formation of bicycle 9aa, while catalytic addition of benzoic acid as an additive enhanced the efficiency of the transformation in favor of tricyclic product 10aa. Lastly, the catalyst loading had to be maintained at 20 mol% level, since lowering the quantity of catalyst heavily impacted the overall efficiency (Table 1, entry 12, and Table S2 in Supporting Information), clearly suggesting clues on the reaction mechanism (see *infra*).

Overall, the optimized reaction protocol toward bicyclic product 9aa entailed the use of a 2:1 ratio of N,N-dimethyl-substituted 7a and cinnamaldehyde 8a, catalyst C1 with a 20 mol% loading, in the absence of any additives, in dichloromethane at room temperature for 24 h, leading to 9aa in 68% isolated yield, >10:1 chemoselectivity and >99% ee (Table 1, entry 14).

The optimized procedure to tricyclic product 10aa called for the use of uracil 7a and enal 8a in a 1:3 ratio, using the same catalyst C1 in 20 mol% loading, with the addition of catalytic benzoic acid (20 mol%) in dichloromethane at room temperature, giving 10aa in 68% isolated yield, 6:1 chemoselectivity, and >99% ee (Table 1, entry 16).

We next investigated a battery of diversely functionalized substrates 7 and 8 in order to evaluate the functional group compatibility of the two procedures. Table 2 and Table 3 illustrate the results of this investigation toward bicyclic uracils 9 and tricyclic compounds 10, respectively. As for the eliminative [4 + 2] cyclization to products 9, substituted cinnamaldehydes 8 bearing either electron-withdrawing or electron-donating groups proved competent enal substrates in couple with N,N-dimethyl uracil 7a, giving the corresponding bicycles 9ab, 9ac, 9ae, 9af, and 9ah in reasonable-to-good isolated yields and excellent enantioselectivities in all cases. The reaction toward 9ab was repeated on a 5× scale proving equally efficient and enantioselective. Good results were also obtained with naphthyl derivative 9ad and furyl-equipped compound 9ag. Inferior performance was instead witnessed using a polyconjugated dienal substrate (namely, 5-phenyl-2,4-pentadienal 8i), which reacted with 7a giving bicycle 9ai in a poor 20% yield, accompanied by preponderant formation (50% yield) of the corresponding aromatized compound (see Supporting Information). In this case, extended double bond conjugation could be responsible for facile oxidation of 9ai in air during the workup procedure. Variation of the uracil component 7 entailed the use of methoxymethyl- (MOM), methoxyethoxymethyl- (MEM), and benzyloxymethyl- (BOM) substituted uracils 7b, 7c, and 7d, respectively, which were prepared from commercial methyluracil carbaldehyde 6 in three steps (see Supporting Information). These substrates reacted with cinnamaldehyde according to the standard procedure, providing the corresponding products 9ba, 9ca, and 9da in good isolated yields and, again, notable enantiomeric excesses.[12]

As a limitation of the procedure, the reactions failed with N,N-unsubstituted uracil substrate (Table 2), mainly due to its very poor solubility in dichloromethane. Also,  $\beta$ -alkyl-substituted enals (e.g. R2 = cyclohexyl) proved recalcitrant substrates under the reported reaction conditions, even with prolonged

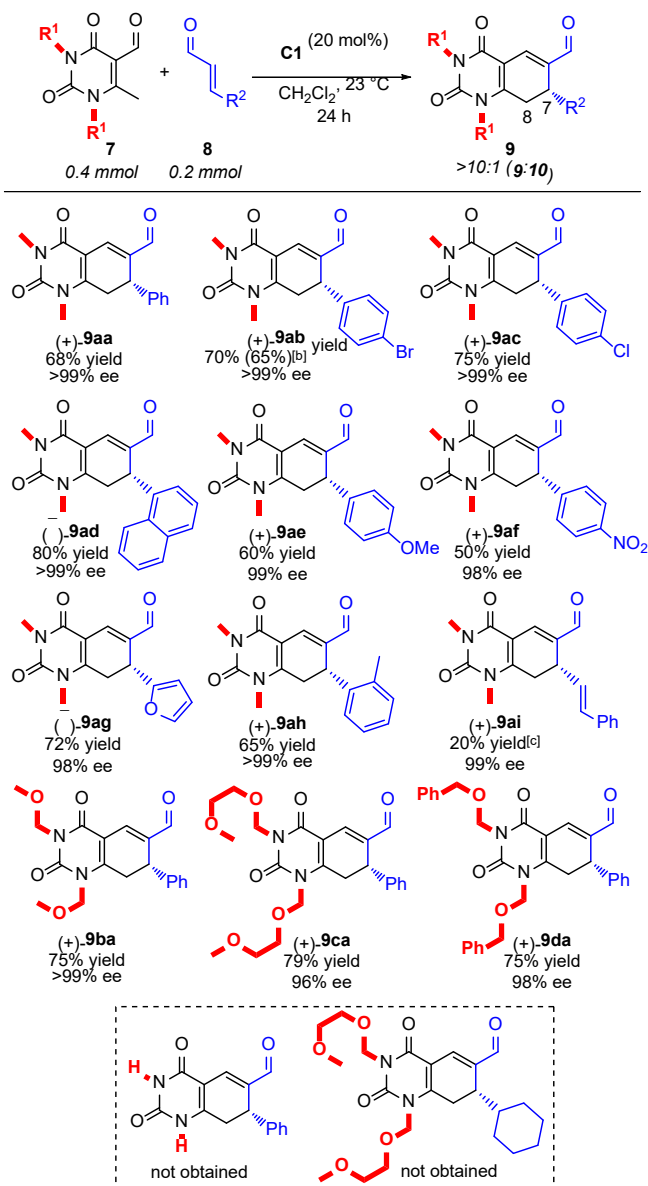
*This item was downloaded from IRIS Università di Bologna (<https://cris.unibo.it/>)*

***When citing, please refer to the published version.***

reaction times and higher temperatures. In all cases reported in Table 2, chemoselectivity between the expected products 9 and the corresponding tricycles 10 remained at high levels (9:10, >10:1), as determined by NMR analysis of the crude reaction mixtures.

By simply adjusting the substrate ratio and adding benzoic acid co-catalyst (optimized conditions of Table 1, entry 16), access to variously adorned products 10 was at hand, which remarkably feature a tricyclic skeleton with six contiguous stereocenters. The representative compounds in Table 3 were obtained in good isolated yields, moderate-to-good chemoselectivity (10:9, 6:1), complete diastereoselectivity, and excellent levels of enantioselectivity, as detected by chiral HPLC analysis of the corresponding bis-carbinols.

Table 2. Substrate scope for the chemo-, regio-, and enantioselective synthesis of bicyclic uracils 9.[a]



[a] All reactions were run under inert atmosphere in 0.1 M solutions of dry CH<sub>2</sub>Cl<sub>2</sub>. Yields refer to isolated products 9. Enantiomeric excesses (ee) were determined by HPLC analysis on a chiral stationary phase. [b]

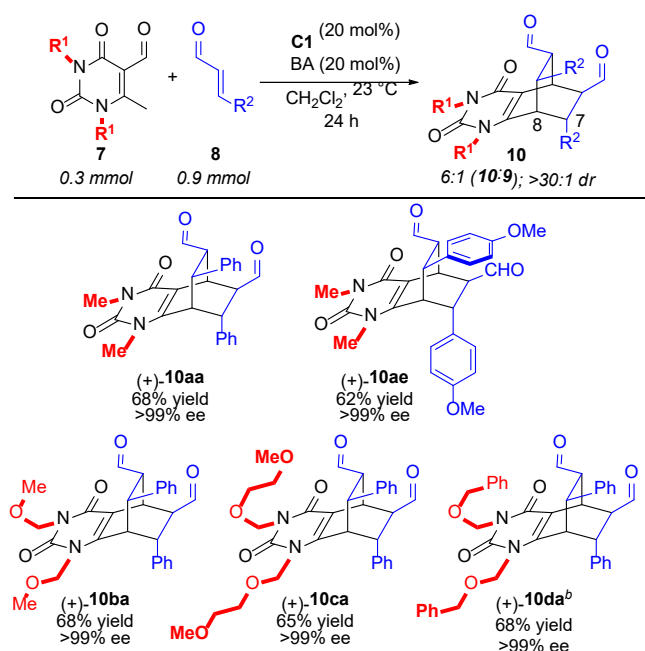
This item was downloaded from IRIS Università di Bologna (<https://cris.unibo.it/>)

When citing, please refer to the published version.

Isolated yield on a 5 × scale. [c] The corresponding aromatized achiral product was isolated in 50% yield. For further details, see the Supporting Information.

The varied functional group pattern of compounds 9 and 10 served for further chemical transformations. Derivatization of aldehyde ent-9ae into crystalline benzoyl carbinol 11 (Scheme 3, eq. 1), allowed us to determine the absolute configuration of the products indirectly, by single crystal X-ray analysis (see the Supporting Information for details).[13] Further elaborations included carbonyl reduction of products 10 into the corresponding bis-alcohols 12 (Scheme 3, eq. 2), and reductive removal of BOM protections from bis-carbinol 12da to afford N,N-unsubstituted tricycle 13da (eq. 3).

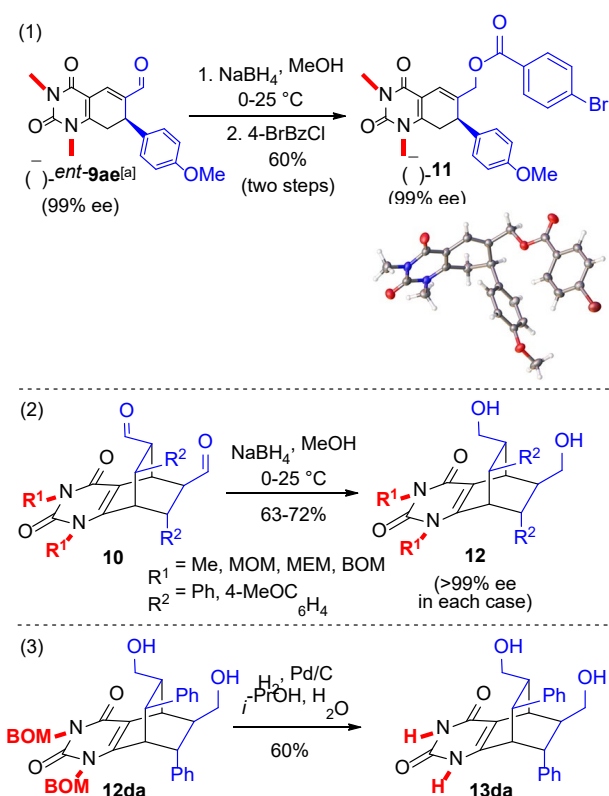
Table 3. Substrate scope for the chemo-, regio-, diastereo-, and enantioselective synthesis of tricyclic uracils 10.[a]



[a] All reactions were run under inert atmosphere in 0.1 M solutions of dry CH<sub>2</sub>Cl<sub>2</sub>. Yields refer to isolated products 10. Diastereomeric ratios (dr) were determined by <sup>1</sup>H NMR analysis of the crude reaction mixtures. Enantiomeric excesses (ee) were determined by HPLC analysis of the corresponding bis-alcohols of type 12 (see infra, Scheme 3) using a chiral stationary phase. [b] Relative configuration corroborated by 2D NMR NOESY analysis (CDCl<sub>3</sub>, 400 MHz). For further details, see the Supporting Information.

This item was downloaded from IRIS Università di Bologna (<https://cris.unibo.it/>)

**When citing, please refer to the published version.**



Scheme 3. Chemical elaboration of the fused uracil products. MOM = methoxymethyl, MEM = methoxyethoxymethyl, BOM = benzyloxymethyl. For experimental details, see the Supporting Information. [a] Obtained from 7a and p-methoxycinnamaldehyde (8e) according to the conditions reported in Table 2, using ent-C1 instead of C1.

**Mechanistic Insights.** The chemistry herein disclosed posed questions about the actual mechanism of these transformations, and special investigation was deserved to unravel three central points: i) role played by the amine catalyst in orchestrating the coupling between the substrates; ii) nature of the eliminative [4 + 2] cross cycloaddition to bicycles 9 (i.e. concerted vs stepwise, catalyst recycling via elimination); iii) nature of the double [4 + 2] cycloaddition sequence to tricycles 10 and possible linking between the bicycle/tricycle catalytic cycles.

i) About the role played by the amine catalyst. From the observed experimental results, we learnt that C1 was an indispensable ingredient for the reaction to occur, enantiocontrol was almost excellent in all cases, and decreasing catalyst loading to less than 20 mol% dramatically lowered the efficiency of the process, giving clues about a double participation of the catalyst in activating both substrates. Given the poorly differentiated nature of the starting reactants 7 and 8 (both  $\alpha,\beta$ -unsaturated aldehydes), it was reasonable to assume a concomitant covalent activation of both 7 and 8 by the aminocatalyst. Organocatalyzed cross- or self-condensations of aldehydes are known in literature, but in-depth studies supported by calculations and/or experimental evidences about their mechanism are quite rare and could hardly help us in this endeavor.<sup>[14]</sup> In order to test the hypothesis that a double activation of reactants by C1 was operative, a couple of control experiments was carried out, where either of the two reactants was replaced by a non-aldehyde non-activatable congener (Scheme 4, eqs. 1 and 2). Thus, when 7a was reacted with E-nitrostyrene (14) in the presence of C1 (20 mol%), the corresponding bicyclic compound 15 was isolated in

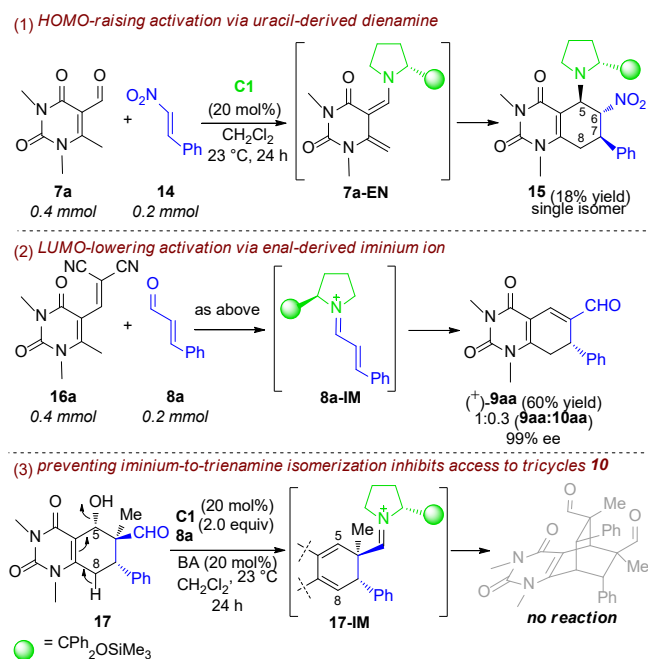
This item was downloaded from IRIS Università di Bologna (<https://cris.unibo.it/>)

**When citing, please refer to the published version.**

18% yield as a single diastereoisomer (Scheme 4, eq. 1). Incorporation of the catalyst moiety within the framework of the final product clearly established the role of dienamine intermediate 7a-EN in the addition reaction, thus confirming the hypothesis that uracil-based aldehyde 7a may be activated by C1 via dienamine formation. More detailed investigation of this control reaction via DFT calculations[15] showed that this cycloaddition reaction proceeds via a two-step mechanism entailing a first rate- and stereo-determining dienamine-mediated vinylogous Michael reaction to fix the C7-C8 bond, followed by closure of the nitronate intermediate to the evolving iminium ion to install the C5-C6 bond (see Chart S2 in the Supporting Information).

In the second control experiment (Scheme 4, eq. 2), uracil aldehyde 7a was converted into alkenylidene malononitrile 16a, which was reacted with cinnamaldehyde 8a under the usual optimized conditions. In the event, bicyclic product 9aa was mainly recovered in excellent enantiocontrol (99% ee), thus corroborating the hypothesis of an active participation of catalyst C1 in this reaction, via iminium ion 8a-IM (in this instance, a [4 + 2] cycloaddition followed by elimination of malononitrile is operative).[10b] Further confirmation of this hypothesis came from DFT calculations, as described in the next paragraph.

ii) About the nature of the eliminative [4 + 2] cross cycloaddition toward bicycles 9. Given the reasonable existence of both 7a-EN and 8a-IM in the reaction context, we initially modelled the addition reaction of 7a-EN to the iminium ion 8a-IM (Chart 1). DFT calculations[15] revealed a two-step reaction mechanism but, contrary to the previously calculated pathway (Scheme 4, eq. 1 and Chart S2 in Supporting Information), now the second C5-C6 bond-forming reaction determines the overall cyclization barrier.



Scheme 4. Control experiments supporting the mechanistic investigation.

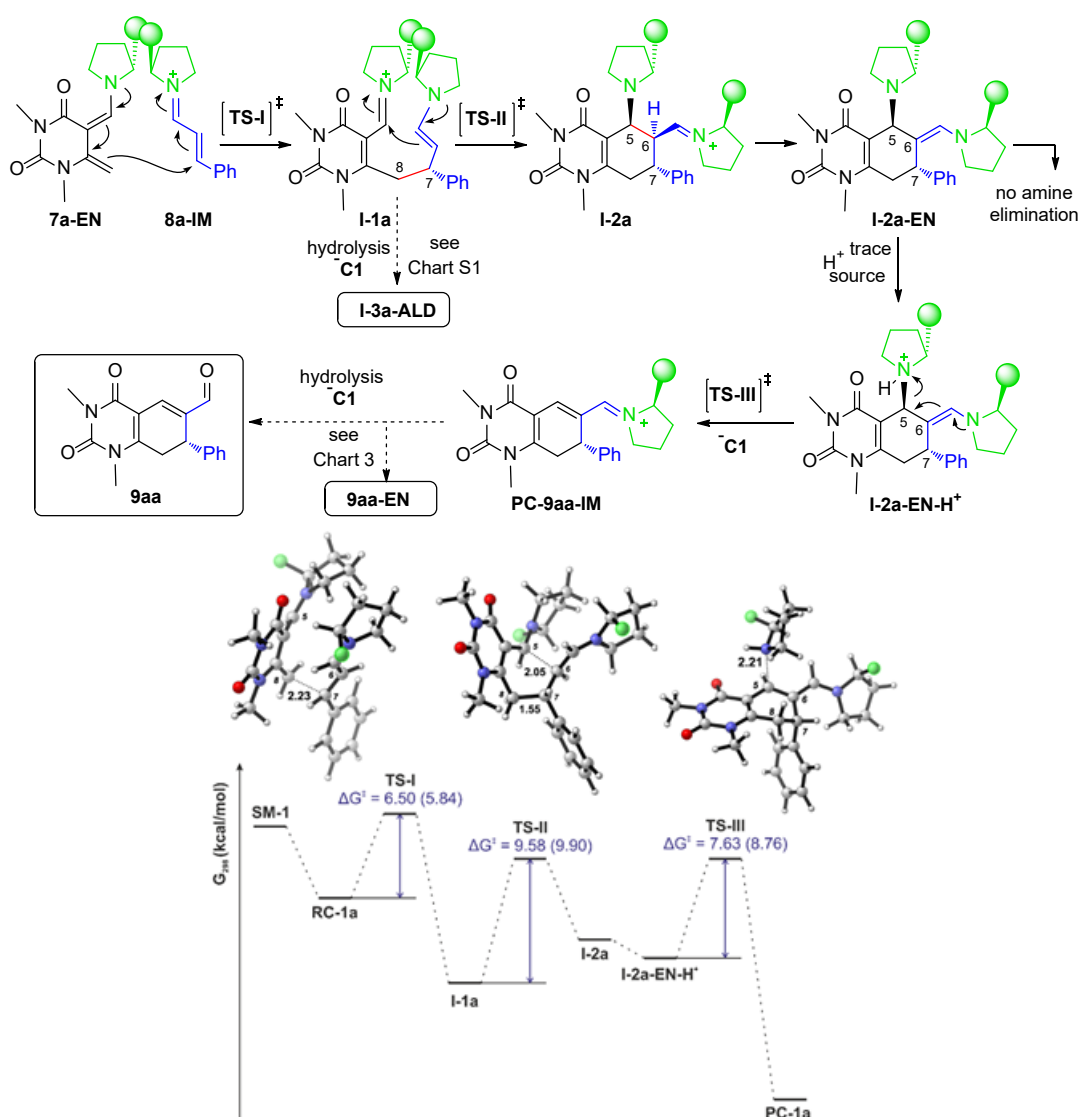
In this case, both the dienamine 7a-EN and the Michael acceptor 8a-IM possess a single unhindered diastereotopic face available for the addition. As a result, a single approach of the two reagents becomes energetically feasible, determining the (S)-absolute configuration of the C7 stereocenter of the target. The reaction profile for the complete cyclization deriving from the most favorable synclinal approach of 7a-EN and 8a-IM and leading to the iminium ion of the final product 9aa is reported in Chart 1. The structures of

This item was downloaded from IRIS Università di Bologna (<https://cris.unibo.it/>)

**When citing, please refer to the published version.**

transition states relative to C7-C8 (TS-I) and C5-C6 (TS-II) bond-forming reactions, as well as the transition state for the elimination reaction (TS-III) are also depicted in Chart 1. While the iminium ion moiety within intermediate I-2a could be in principle hydrolyzed releasing half of the bound catalyst C1, the part directly bound to C5 cannot readily re-enter the catalytic cycle. In order to establish whether the final eliminated product 9aa could be formed from this intermediate, we tried to model the elimination reaction from the enamine I-2a-EN deriving from I-2a, but no feasible reaction pathway could be found. Indeed, a possible elimination pathway was found from enamine I-2a-EN-H<sup>+</sup> bearing a protonated pyrrolidine ring at C5 (Chart 1). A possible explanation could be that, even in the absence of acidic additives, catalytic amounts of protic acids are still present in solution, due to easy oxidation of the commercially available starting aldehydes.

A second explanation for the different behavior of cinnamaldehyde 8a with respect to nitrostyrene 14 could be found in the different energetic requirement for the final cyclization step. While the nitronate ion cyclizes almost with no barrier (I-7 in Chart S2), ring closure of intermediate I-1a is considerably more energetically demanding (Chart 1), rendering iminium hydrolysis before the cyclization step possible.



This item was downloaded from IRIS Università di Bologna (<https://cris.unibo.it/>)

When citing, please refer to the published version.

Chart 1. Reaction scheme (above) and reaction profile (below) for the addition of 7a-EN to 8a-IM. Free energy profiles (kcal·mol<sup>-1</sup>) in the gas-phase at the M06-2X/6-31G(d) level of theory. Energies in parentheses are relative to single point calculations at the M06-2X/6-311++G(d,p) level of theory in CH<sub>2</sub>Cl<sub>2</sub>. SM-1: separated reactants at infinite distance (7a-EN + 8a-IM); RC: reactant complex; TS: transition state; I: intermediate; PC-1a: product complex (9aa-IM + C1). Structures of transition states TS-I (synclinal approach), TS-II (cyclization step) and TS-III (elimination reaction); distances in Angstrom. Silylated diphenylmethanol group is represented as a green sphere.

In order to establish whether this last reaction pathway is possible, we modeled the corresponding cyclization/elimination steps on the aldehyde deriving from intermediate I-1 (I-3a-ALD, see Chart S1, Supporting Information). The calculated reaction profiles for the cyclization reactions are in complete accordance to those reported by Houk for the aldol reaction between acetaldehyde and N,N-dimethylvinylamine.[16] In particular, in the absence of acidic additives, the reaction proceeds to give an oxetane intermediate with a large activation barrier (40.0 kcal·mol<sup>-1</sup> in the gas phase and 31.6 kcal·mol<sup>-1</sup> in CH<sub>2</sub>Cl<sub>2</sub>); on the contrary, in the presence of a protic acid, the cyclization step proceeds promptly without any barrier. Similarly to what observed for I-2a (Chart 1), no further elimination reaction could be found in the absence of a proton source. Upon protonation of the cyclized alcohol intermediate, a transition state leading to the iminium ion of the final product was easily identified, by starting from either E- or Z-configured enamine (Chart S1, Supporting Information). Differently from amine elimination, where the iminium ion/enamine conversion was almost an isoergonic transformation (I-2a/I-2a-EN, Chart 1,  $\Delta G_{298} = -1.4$  kcal·mol<sup>-1</sup> in the gas phase and 0.12 kcal·mol<sup>-1</sup> in CH<sub>2</sub>Cl<sub>2</sub>), in this latter case the same conversion was highly endergonic ( $\Delta G_{298} = 22.9/23.3$  kcal·mol<sup>-1</sup> in the gas phase and 20.8/24.7 kcal·mol<sup>-1</sup> in CH<sub>2</sub>Cl<sub>2</sub>, for E- and the Z-enamines, respectively), suggesting a quite large activation barrier.

Finally, to confirm the involvement of 8a-IM in the reaction course, the addition of 7a-EN to 8a was also modeled (Chart 2). In this case, a single-step asynchronous cyclization was found, characterized by a transition state (TS-IV) in which the C7-C8 bond is almost formed (2.09 Å), while the C5-C6 bond is considerably longer (2.89 Å). Moreover, the corresponding activation barrier (15.8 kcal·mol<sup>-1</sup> in the gas phase and 13.6 kcal·mol<sup>-1</sup> in CH<sub>2</sub>Cl<sub>2</sub>) resulted more than doubled than that relative to the addition to 8a-IM (see Chart 1 vs Chart 2).

So far, the calculation results suggested that 1) the addition reaction definitely involves both the enamine of 7a and the iminium ion of 8a derived from condensation with catalyst C1, constituting a perfect yet rare example of a very efficient enantioselective homo-synergistic organocatalytic transformation. Indeed, amine-catalyzed eliminative [4 + 2] cycloadditions were previously reported by Watanabe[14a] and Jorgensen groups,[14c] dealing with self- or cross condensation of linear enals; in those instances, double activation of both substrates via enamine and iminium ion formation with the organocatalyst was postulated, but only partial investigation of the actual reaction mechanism was documented. 2) The presence of traces of a protic acid is required to foster the final elimination reaction, and 3) even if the acid-catalyzed cyclization step involving the aldehyde acceptor is considerably faster than the addition to the corresponding iminium ion (Chart S1 vs Chart 1), the subsequent iminium/enamine isomerization, required for the final elimination step, appears much more energetically favorable in the case of the iminium ion pathway (Chart 1).

*This item was downloaded from IRIS Università di Bologna (<https://cris.unibo.it/>)*

***When citing, please refer to the published version.***



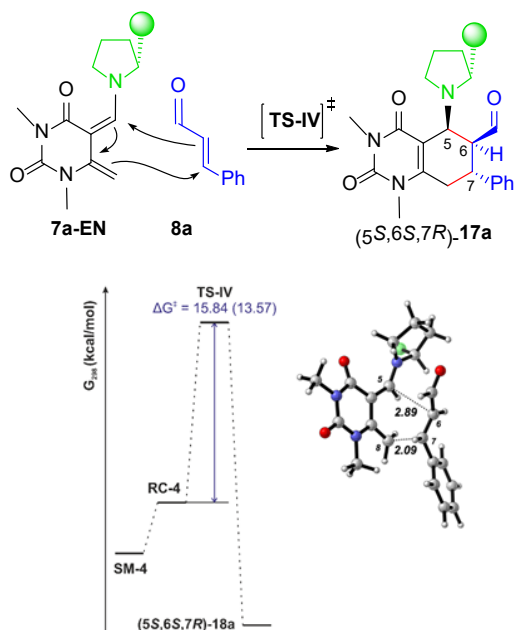


Chart 2. Reaction scheme (above), reaction profile (below, left) for the addition of 7a-EN to 8a and structure of transition state TS-IV (below, right, distances in Angstrom). Free energy profiles (kcal·mol<sup>-1</sup>) in the gas-phase at the M06-2X/6-31G(d) level of theory. Energies in parentheses are relative to single point calculations at the M06-2X/6-311++G(d,p) level of theory in CH<sub>2</sub>Cl<sub>2</sub>. SM-4: separated reactants at infinite distance; RC: reactant complex; TS: transition state. Silylated diphenylmethanol group is represented as a green sphere.

iii) About the nature of the double [4 + 2] cycloaddition sequence to tricycles 10 and possible linking between the bicycle/tricycle catalytic cycles. As described in the synthesis paragraph, when the reaction was carried out in the absence of additives and with a slight excess of uracil 7a (1.5 equiv), product 9aa was isolated in good overall yield, together with trace amounts of tricyclic adduct 10aa (Table 2, entry 9, non-optimized conditions). Indeed, when the reaction was carried out in the same conditions in the presence of 20 mol% benzoic acid as an acidic additive (Table 2, entry 13), 9aa and 10aa were isolated in comparable yields. These results suggested that 10aa derives directly from an intermediate involved in the formation of 9aa. Thus, under optimized conditions (Table 2, entry 16), 10aa could be isolated as the main reaction product if the catalytic cycle is fostered by an acidic additive and a larger excess of cinnamaldehyde 8a is used (3 equiv). Considering the mechanistic rationale so far obtained, it seems reasonable to postulate that the trienamine 9aa-EN - directly deriving by isomerization of the iminium ion 9aa-IM (the final product in Chart 1) - is involved in a further coupling to the iminium ion of cinnamaldehyde (8a-IM), leading to the formation of 10aa (Chart 3). DFT calculations showed, once more, that this reaction follows a two-step mechanism, where the second step, namely the cyclization reaction, determines the overall reaction barrier. Again, both trienamine 9aa-EN and the Michael acceptor 8a-IM have only one unhindered diastereotopic face available for the addition, completely determining the (8R,9S)-absolute configuration of the newly forged C8 and C9 stereocenters. Accordingly, the second cyclization step fixes the absolute (5S,10S)-configuration at the C5 and C10 stereocenters in an unequivocal manner. The overall [4 + 2] cycloaddition entails a first trienamine-mediated bisvinyllogous Michael reaction, followed by an intramolecular enamine-mediated Michael reaction; in the event, four new contiguous stereocenters are nicely formed with complete absolute stereocontrol. The configuration of the last new stereocenter at the

This item was downloaded from IRIS Università di Bologna (<https://cris.unibo.it/>)

**When citing, please refer to the published version.**



C6 position is determined later, during enamine/iminium ion equilibration to consign the final target 10aa; the aldehyde substituent at C6 assumes the most thermodynamically stable pseudo-equatorial disposition, thus accounting for the observed 6S-absolute configuration for this stereocenter.

Given the above considerations, chemodivergence toward either bicyclic product 9aa or tricyclic congener 10aa is established by the presence of the key oQDM-like trienamine intermediate 9aa-EN directly deriving from 9aa-IM. If conditions are present which favor this isomerization (e.g. protic conditions), the reaction proceeds to tricycle 10aa, especially when excess of dienophile 8a-IM is present. On the other hand, if 9aa-IM is not given the possibility to isomerize to trienamine 9aa-EN, for instance because it is hydrolyzed to the corresponding aldehyde, then the reaction path stops at this stage consigning bicycles 9. As a confirmation of this sentence, one further control experiments was carried out (Scheme 4, eq. 3), where bicyclic compound 17, bearing a quaternary C6 carbon, was reacted with cinnamaldehyde 8a in the presence of catalyst C1 and benzoic acid (20 mol% each). In the event, no even minimal conversion of 17 to the corresponding tricyclic compound was witnessed in 24 h. In this case, transformation of 17 to the corresponding oQDM would be in principle possible via 5,8-conjugate water elimination, but no isomerization to the trienamine would be feasible due to interruption of conjugation by the quaternary C6 center, with consequent inhibition of the [4 + 2] cyclization to any tricyclic product. That is to say, only hypervinylogous enamines of type 9aa-EN may succeed to forge such complex tricyclic structures, providing chemodivergence.

An overall depiction of the intertwined catalytic cycles accounting for the transformations outlined in this work is given in Scheme 5.

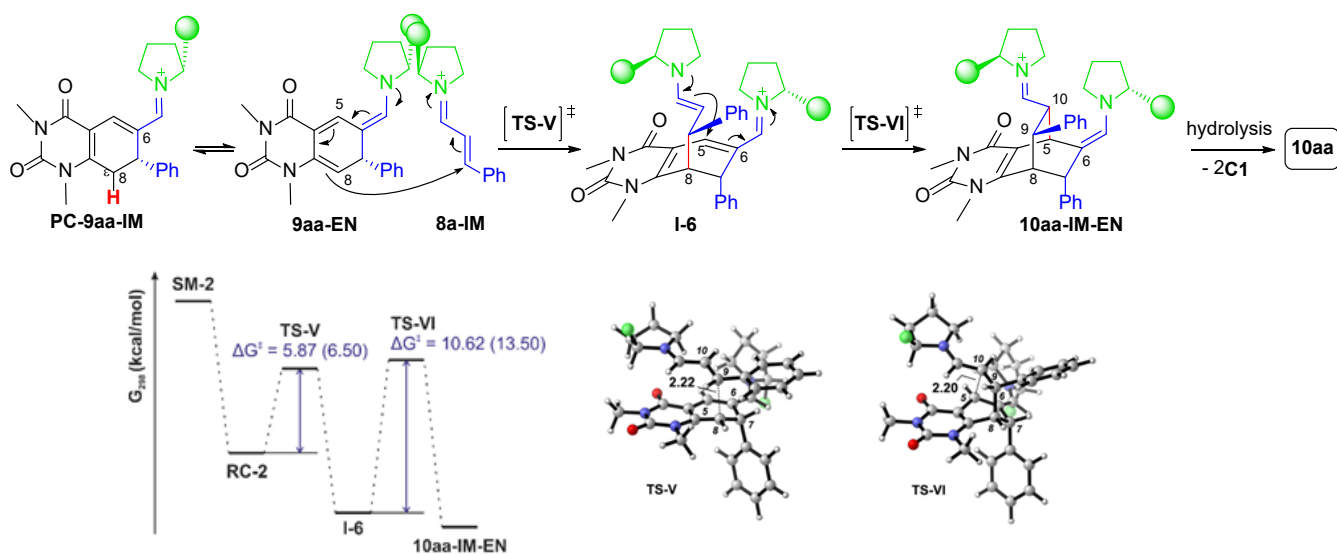
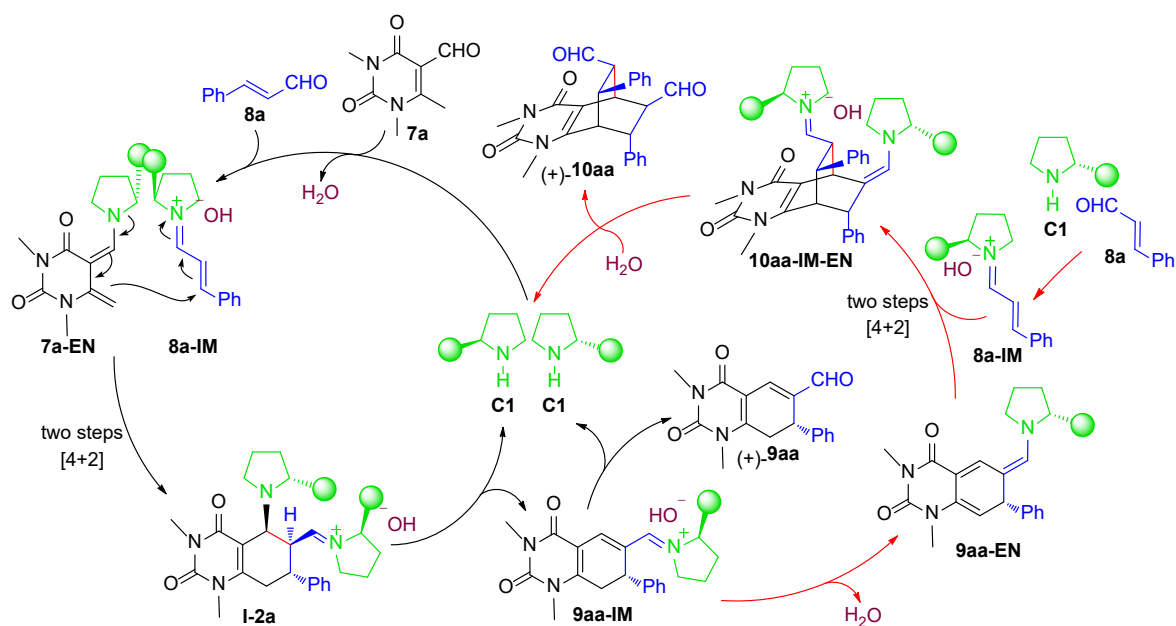


Chart 3. Reaction scheme (above) and reaction profile (below) for the addition of 9aa-EN to 8a-IM. Free energy profiles (kcal·mol<sup>-1</sup>) in the gas-phase at the M06-2X/6-31G(d) level of theory. Energies in parentheses are relative to single point calculations at the M06-2X/6-311++G(d,p) level of theory in CH<sub>2</sub>Cl<sub>2</sub>. SM-2: separated reactants at infinite distance (9aa-EN + 8a-IM); RC: reactant complex; TS: transition state; I: intermediate. Transition state TS-V (addition reaction) and TS-VI (cyclization reaction); distances in Angstrom. Silylated diphenylmethanol group is represented as a green sphere.

This item was downloaded from IRIS Università di Bologna (<https://cris.unibo.it/>)

**When citing, please refer to the published version.**



Scheme 5. Organocatalytic homo-synergistic cycles 1 (black arrows) and 2 (red arrows) accounting for the chemodivergent synthesis of bicycles 9 and tricycles 10 in this study.

## Conclusion

A novel method has been developed, which allowed the rapid transformation of easily accessible and low-cost uracil substrates of type 7 to new three-dimensional carbocycle-fused uracils. The rationale behind this endeavor was simple: installation of a carbaldehyde functional group at the C5 site of 6-methyluracil (as in uracils 7) would enhance the remote enolization at the vinylogous C6-methyl site, favor the formation of a reactive oQDM species (an activated diene) for [4 + 2] coupling to an enal acceptor (dienophile), while providing a possible appendage for the covalent activation by the amine catalyst. The hypothesis was confirmed by real-world chemistry and, upon optimized mild reaction conditions, the route proved practical and chemodivergent, providing access to two distinct small collections of products in good yields and almost complete enantioselectivities namely, bicyclic compounds 9 and tricyclic products 10, remarkably featuring six contiguous stereocenters.

Detailed DFT calculations and control experiments clarified the role of the silylprolinol catalyst, which solely and concomitantly activates both enal substrates and orchestrates the overall transformation. To the best of our knowledge, this is the first example of sound mechanistic investigation proving the homo-synergistic approach by an amine organocatalyst. Mechanistically, a first organocatalyzed stepwise eliminative [4 + 2] cross cycloaddition between the carbaldehyde substrates leads to a bicyclic iminium ion intermediate (PC-9aa-IM), which divergently turns into bicyclic targets 9 by hydrolysis, or converts to tricyclic targets 10 via a further trienammine-mediated stepwise [4 + 2] cycloaddition, depending upon the reaction conditions.

We anticipate that this robust and simple chemical transformation will serve to widen sampling of three-dimensional chemical space around the key uracil core.

## Acknowledgements

This item was downloaded from IRIS Università di Bologna (<https://cris.unibo.it/>)

**When citing, please refer to the published version.**

This work was supported by Regione Autonoma della Sardegna (RASSR81788, 2017, “Green Chemistry in Drug Discovery - sintesi sostenibili di nuovi inibitori di telomerase”) and by Università di Parma (ZNRFC\_RICERCA\_IST). G.P. wishes to thank Chiesi Farmaceutici S.p.A. for the use of D8Venture diffractometer. Thanks are due to Centro Interdipartimentale Misure “G. Casnati” (Università di Parma, Italy) for instrumental facilities.

Keywords: asymmetric synthesis • fused-ring systems • heterocycles • organocatalysis • vinylogy

- [1] Y. Qin, L. Zhu, S. Luo, *Chem. Rev.* 2017, 117, 9433–9520.
- [2] D. C. Blakemore, L. Castro, I. Churcher, D. C. Rees, A. W. Thomas, D. M. Wilson, A. Wood, *Nat. Chem.* 2018, 10, 383–394.
- [3] T. L. P. Galvão, I. M. Rocha, M. D. M. C. Ribeiro da Silva, M. A. V. Ribeiro da Silva, *J. Phys. Chem. A* 2013, 117, 5826–5836.
- [4] S. I. Zav’yalov, G. I. Ezhova, N. E. Kravchenko, L. B. Kulikova, O. V. Dorofeeva, E. E. Rumyantseva, A. G. Zavozin, *Pharm. Chem. J.* 2003, 37, 337–341.
- [5] a) E. De Clercq, *J. Med. Chem.* 2019, 62, 7322–7339; b) A. Pałasz, D. Cież, *Eur. J. Med. Chem.* 2015, 97, 582–611.
- [6] M. I. Lin, B. H. Su, C. H. Lee, S. T. Wang, W. C. Wu, P. Dangate, S. Y. Wang, W. I. Huang, T. J. Cheng, O. A. Lin, Y. S. E. Cheng, Y. J. Tseng, C. M. Sun, *Eur. J. Med. Chem.* 2015, 102, 477–486.
- [7] C. Curti, L. Battistini, A. Sartori, F. Zanardi, *Chem. Rev.* 2020, 120, 2448–2612, and references therein.
- [8] a) B. Yang, S. Gao, *Chem. Soc. Rev.* 2018, 47, 7926–7953; b) B.-X. Xiao, X.-Y. Gao, W. Du, Y.-C. Chen, *Chem. Eur. J.* 2019, 25, 1607–1613.
- [9] Y. Liu, M. Nappi, E. Arceo, S. Vera, P. Melchiorre, *J. Am. Chem. Soc.* 2011, 133, 15212–15218.
- [10] a) G. Rassu, C. Curti, V. Zambrano, L. Pinna, N. Brindani, G. Pelosi, F. Zanardi, *Chem. Eur. J.* 2016, 22, 12637–12640; b) N. Brindani, G. Rassu, L. Dell’Amico, V. Zambrano, L. Pinna, C. Curti, A. Sartori, L. Battistini, G. Casiraghi, G. Pelosi, D. Greco, F. Zanardi, *Angew. Chem.* 2015, 127, 7494–7498; *Angew. Chem. Int. Ed.* 2015, 54, 7386–7390; c) for a recent review on this topic see: C. Curti, A. Sartori, L. Battistini, F. Zanardi, *Synlett* 2018, 29, 266–281.
- [11] T. Li, J. Zhu, D. Wu, X. Li, S. Wang, H. Li, J. Li, W. Wang, *Chem. Eur. J.* 2013, 19, 9147–9150.
- [12] Interestingly, the presence of lipophilic MOM, MEM, and BOM groups at N1/N3 uracil moiety highly impacted the physical properties of both the starting substrates 7 and products 9, which in fact proved much more soluble in organic solvents as compared to the dimethyl-protected counterparts.
- [13] Deposition Number CCDC 1995936 contains the supplementary crystallographic data for this paper. These data are provided free of charge by the joint Cambridge Crystallographic Data Centre and Fachinformationszentrum Karlsruhe Access Structures service [www.ccdc.cam.ac.uk/structures](http://www.ccdc.cam.ac.uk/structures).
- [14] a) B.J. Bench, C. Liu, C.R. Evett, C.M.H. Watanabe, *J. Org. Chem.* 2006, 71, 9458–9463; b) C. Grondal, M. Jeanty, D. Enders, *D. Nat. Chem.* 2010, 2, 167–178; c) N. Hammer, L.A. Leth, J. Stiller, M.E. Jensen, K.A.

*This item was downloaded from IRIS Università di Bologna (<https://cris.unibo.it/>)*

***When citing, please refer to the published version.***

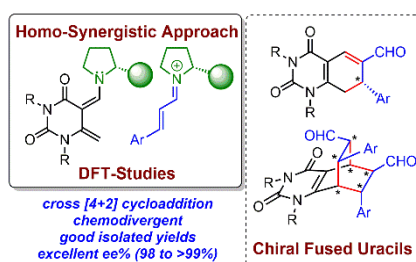
Jørgensen, Chem. Sci. 2016, 7, 3649-3657; d) S. Meninno, M. Meazza, J.W. Yang, T. Tejero, P. Merino, R. Rios, Chem. Eur. J. 2019, 25, 7623–7627.

[15] DFT computational investigation of the relevant reactions involved in this work was carried out at the M06-2X/6-311++g(d,p) IEFPCM (CH<sub>2</sub>Cl<sub>2</sub>)//M06-2X/6-31G(d) level of theory. For details, see Supporting Information.

[16] S. Bahmanyar, K.N. Houk, J. Am. Chem. Soc. 2001, 123, 11273-11283.

Entry for the Table of Contents

Insert graphic for Table of Contents here. ((Please ensure your graphic is in one of following formats))



In synergy to diverge. Cross [4 + 2] cycloadditions between uracil-based aldehydes and  $\alpha$ -aryl enals were carried out under mild conditions in the presence of the popular diphenylsilyl-protected prolinol organocatalyst, which provided homo-synergistic activation of both substrates. Bicyclic and tricyclic fused uracils were chemodivergently forged in good yields and maximum levels of enantioselectivity.

Università di Parma Twitter username: @unipr

This item was downloaded from IRIS Università di Bologna (<https://cris.unibo.it/>)

**When citing, please refer to the published version.**